Electronic Supplementary Material (ESI) for Journal of Materials Chemistry A.
This journal is © The Royal Society of Chemistry 2017

Supporting Infromation

Hollow Nanocubes Composed of Well-dispersed Mixed Metal-rich Phosphides in N-doped Carbon as Highly Efficient and Durable Electrocatalysts for Oxygen Evolution Reaction at High Current Densities

Lei Zhang, Chun Chang, Chan-Wei Hsu, Chih-Wen Chang, Shih-Yuan Lu*

Experimental Section

Materials:

Nickel (II) sulfate hexahydrate ($NiSO_4 \cdot 6H_2O$), potassium hexacyanoferrate (III) ($K_3[Fe(CN)_6]$), trisodium citrate dihydrate ($Na_3C_6H_5O_7 \cdot 2H_2O$), tetraethyl orthosilicate (TEOS), sodium hypophosphite ($NaH_2PO_2 \cdot H_2O$), methanol, ethanol, and ammonium hydroxide were purchased from Sigma-Aldrich. All the reagents were of analytical grade and used as received.

Materials preparation:

***Preparation of $Ni_3[Fe(CN)_6]_2 \cdot H_2O$ nanocube*:** Typically, 0.006 mol of $NiSO_4 \cdot 6H_2O$ and 0.0075 mol of $Na_3C_6H_5O_7 \cdot 2H_2O$ were dissolved in 590 mL of deionized water to form solution A. Then, 0.004 mol of $K_3[Fe(CN)_6]$ was dissolved in 10 mL of deionized water to form solution B. Solutions A and B were thoroughly mixed under magnetic stirring for precipitation, followed by 24 h aging. The precipitates were collected with a centrifuge, washed with deionized water and absolute ethanol five times, and then dried in vacuum at 50 °C for 24 h.

***Preparation of SiO_2 coated $Ni_3[Fe(CN)_6]_2 \cdot H_2O$ nanocube*:** An amount of 0.3 g of $Ni_3[Fe(CN)_6]_2 \cdot H_2O$ nanocubes were dispersed in 160 mL of ethanol under sonication. Ten

milliliters of ammonium hydroxide, 6 mL of methanol, and 1.2 mL of TEOS were added in turn into the suspension slowly. The resulting suspension was aged for 4 h at room temperature under magnetic stirring. The precipitates were collected with a centrifuge, washed with deionized water and absolute ethanol five times, and then dried in vacuum at 70 °C overnight.

Preparation of N doped C/Ni_5P_4/Fe_3P hollow nanocube: Three grams of NaH_2PO_2 and 0.3 g of SiO_2 coated $Ni_3[Fe(CN)_6]_2 \cdot H_2O$ nanocubes were loaded separately into two porcelain boats, and the two precursor-containing boats were situated side by side at the center of a tube furnace with the NaH_2PO_2-containing boat being placed upstream. The calcination was conducted at 400 °C for 4 h with a heating rate of 5 °C min^{-1} under N_2 atmosphere, followed by cooling to ambient temperature under N_2 gas flow. The SiO_2 shell of the product was removed with etching in a 1 wt% HF solution for 24 h. For preparation of N-doped C coated Ni_5P_4/Fe_3P nanoparticles, $Ni_3[Fe(CN)_6]_2 \cdot H_2O$ nanocubes served as the starting material instead of SiO_2 coated $Ni_3[Fe(CN)_6]_2 \cdot H_2O$ nanocubes, following the same procedures as above without the unnecessary HF etching step.

Materials Characterizations:

The composition and crystalline phase of the sample were investigated with powder X-ray diffraction measurements (XRD, Shimadzu XRD-6000, Japan), X-ray photoelectron spectroscopy (XPS, Thermo ESCALAB 250XI, America), energy dispersive spectrometry (EDS, Hitachi S-4800, Japan), and selected area electron diffraction (JEM-2100, Japan). The morphology and microstructure of the product were observed with a scanning electron microscope (SEM, Hitachi S-4800, Japan) and a high resolution transmission electron microscope (TEM, JEM-2100, Japan). Raman spectra were recorded at room temperature in the spectral range of 1000-2000 cm^{-1} using a

Raman spectromicroscope (LabRAM HR800, Horiba Jobin Yvon, France). The specific surface areas of the samples were determined from the N_2 sorption/desorption isotherms, based on the Brunauer-Emmett-Teller model, measured with a Micrometrics ASAP 2010.

Electrochemical characterizations:

The electrochemical performances of the samples were characterized on a CHI6275D electrochemical workstation in a three-electrode system. The working electrode was prepared using the as-prepared powders (85 wt%) as the active material and polyvinylidene fluoride (15 wt%) as the binder. They were mixed in N-methylpyrrolidone (NMP) to form a sample suspension. The working electrode was fabricated by drop-casting the sample suspension, sonicated for 30 min before use, onto a graphite electrode (1 cm × 1 cm) and dried at 80 °C in an oven. The mass loading of the active material on the working electrode was controlled to be around 0.5 mg/cm^2. A platinum foil counter electrode and an Hg/HgO reference electrode were employed to complete the three-electrode system. For the measurements, 1 M KOH (pH = 13.7) aqueous solution was used as the electrolyte. Potentials reported in this study were converted to values referring to the reversible hydrogen electrode (RHE) using the equation $E_{RHE} = E_{Hg/HgO} + 0.118 + 0.059pH$, where $E_{Hg/HgO}$ is the applied potential against the Hg/HgO reference electrode. All the current densities were iR-corrected. The over-potential (η) was calculated using the equation: $\eta = E_{RHE} - 1.23$. Prior to electrochemical measurements, the working electrode was conditioned by cycling through the potential window of 0 to 0.8 V *vs*. Hg/HgO thirty times at a scan rate of 100 mV/s. The polarization curves were recorded with a linear potential sweep at a scan rate of 10 mV/s. The electrochemical impedance spectroscopy measurements were conducted in the same set up from 10^5 to 0.01 Hz with an AC amplitude of 5 mV. The double layer capacitance (C_{dl}), which is

linearly proportional to the electrochemical active surface areas (ECSA) of the catalysts, was measured to estimate the ECSA of the catalyst. The C_{dl} values were determined from the cyclic voltammograms recorded at non-Faradaic potentials (0.83-1.03 V *vs*. RHE) at increasing scan rates. The C_{dl} was obtained as the slope of the capacitive current density (at 0.95 V vs. RHE) vs. scan rate curve.

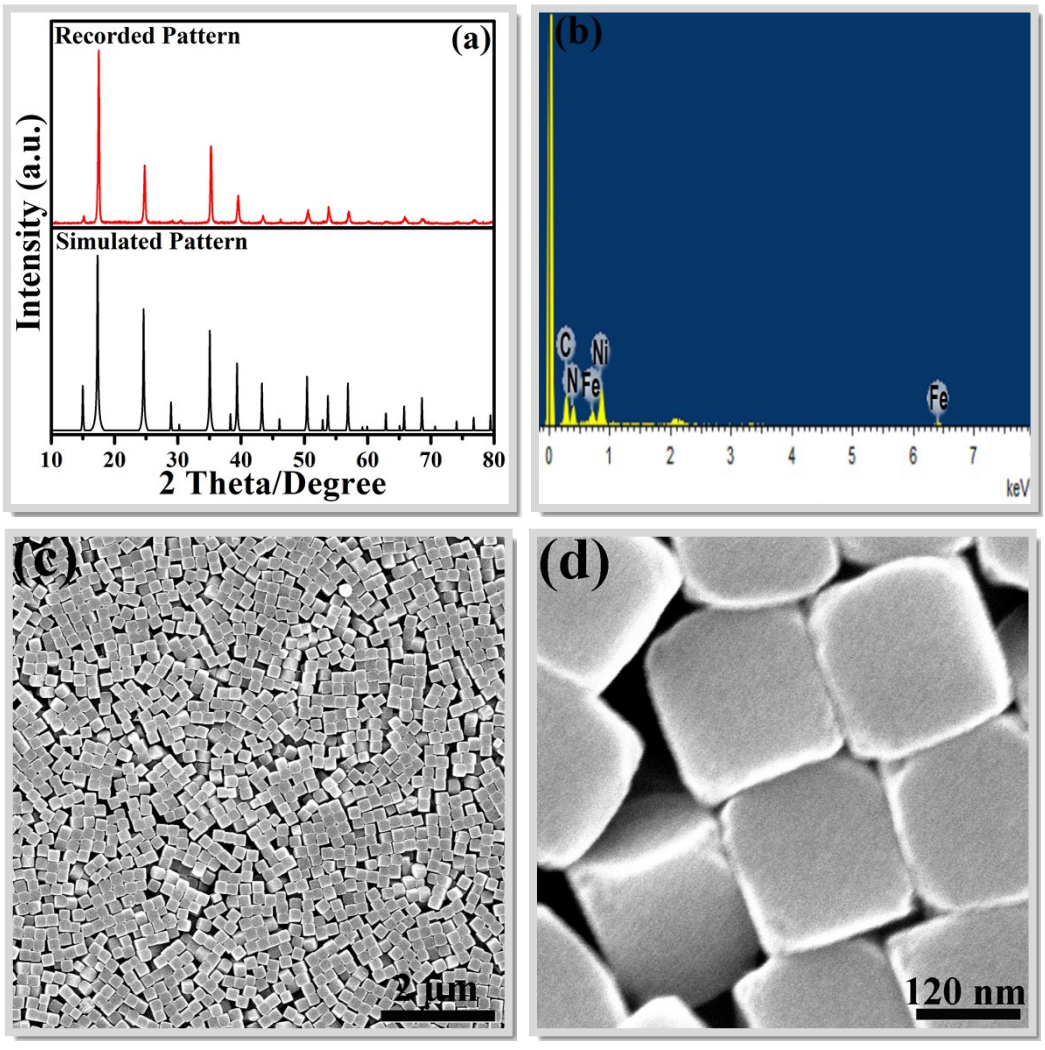

Figure S1 (a) XRD pattern, (b) EDS spectrum, and (c-d) SEM images of as-prepared $Ni_3[Fe(CN)_6]_2 \cdot H_2O$ nanocubes.

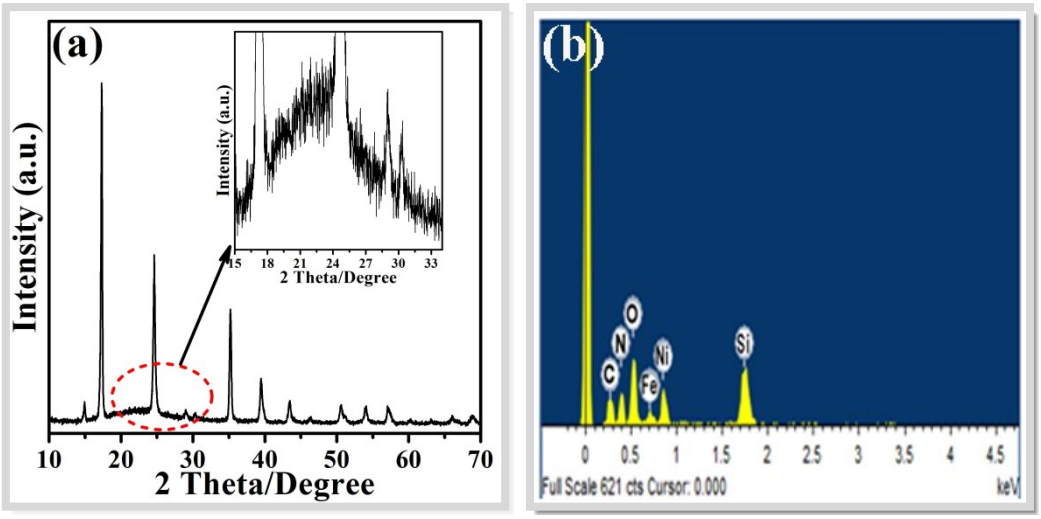

Figure S2 (a) XRD pattern and (b) EDS spectrum of SiO_2 coated $Ni_3[Fe(CN)_6]_2 \cdot H_2O$ nanocubes.

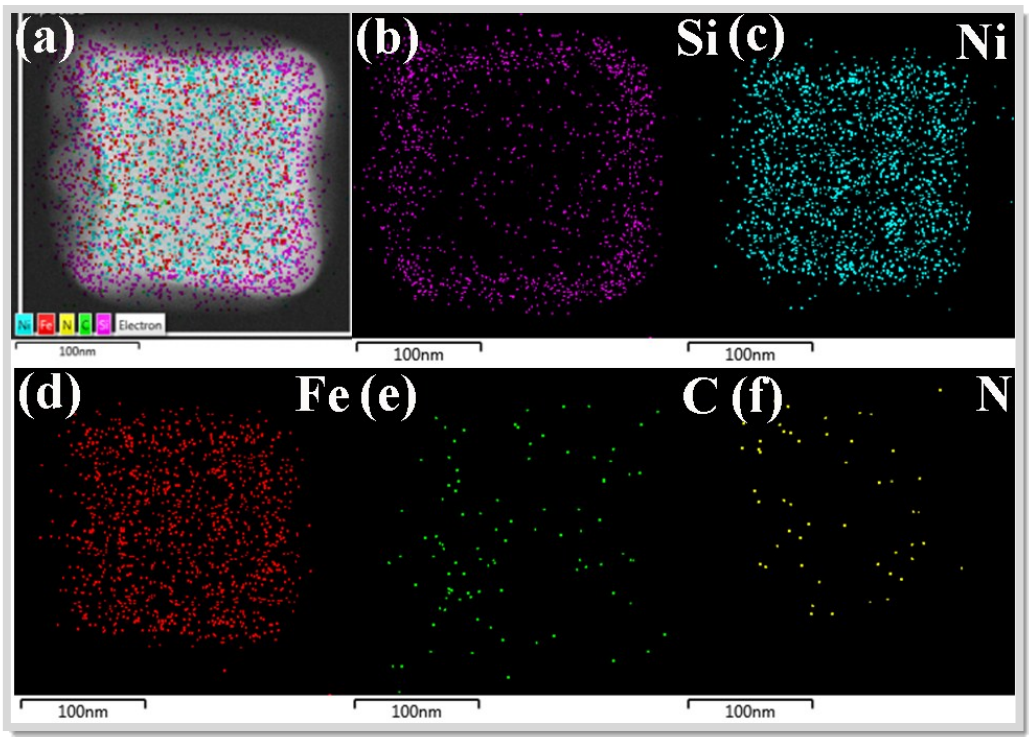

Figure S3 EDS elemental mapping images of SiO_2 coated $Ni_3[Fe(CN)_6]_2 \cdot H_2O$ nanocubes: (a) composite, (b) Si, (c) Ni, (d) Fe, (e) C, and (f) N.

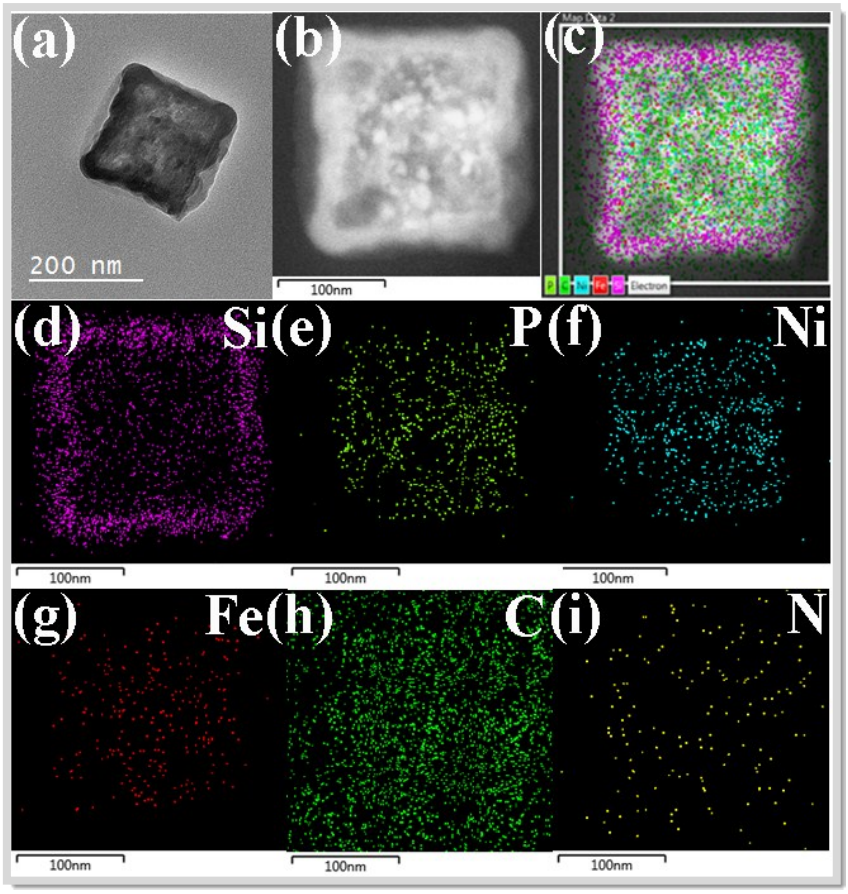

Figure S4 (a) TEM and (b) high-angle annular dark-field scanning transmission electron microscopy images, and EDS elemental mapping images of SiO_2 coated N-doped C/Ni_5P_4/Fe_3P hollow nanocubes: (c) composite, (d) Si, (e) P, (f) Ni, (g) Fe, (h) C, and (i) N.

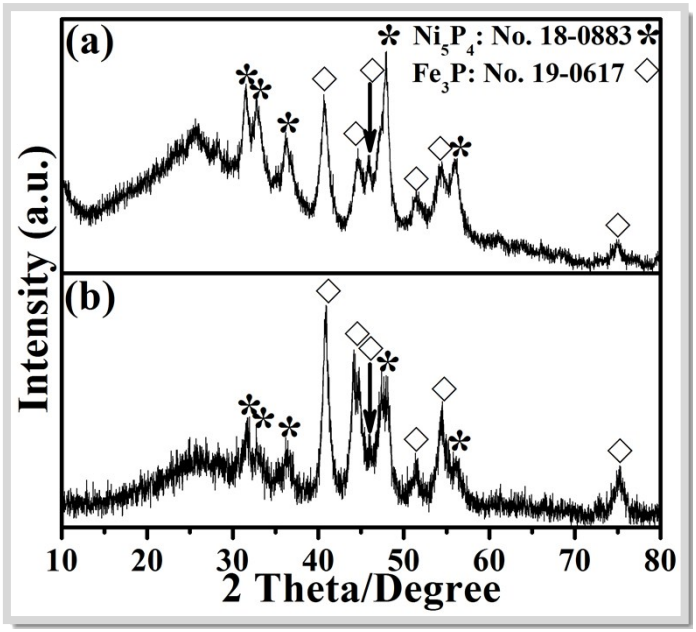

Figure S5 XRD patterns of (a) N-doped C/Ni_5P_4/Fe_3P hollow nanocubes and (b) N-doped C coated Ni_5P_4/Fe_3P nanoparticles.

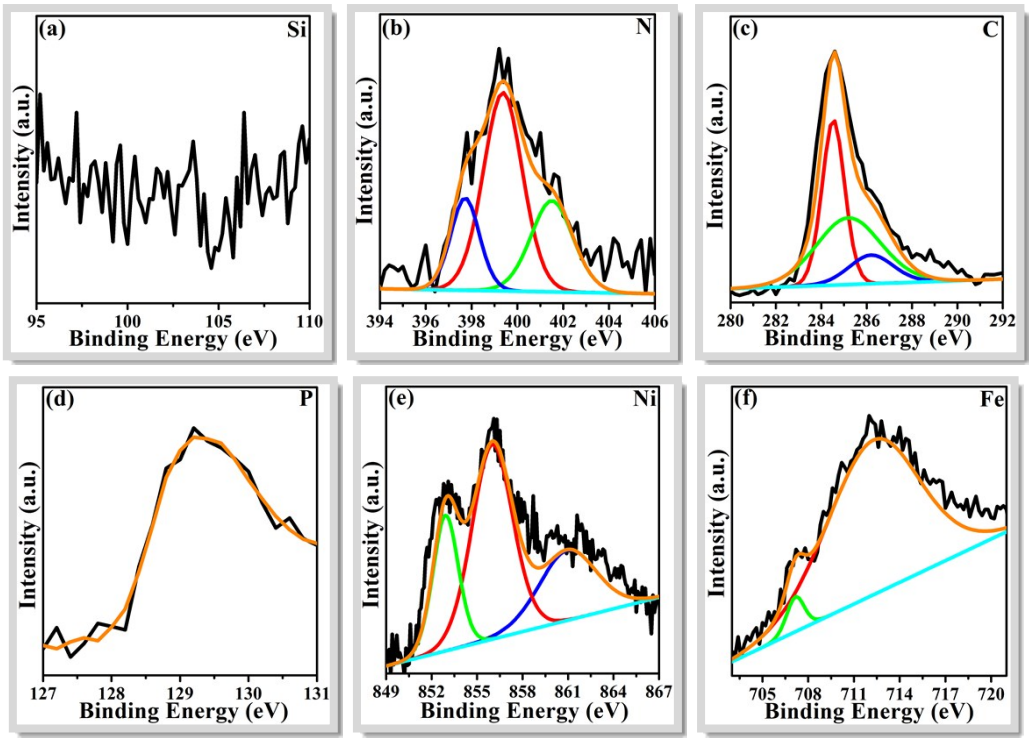

Figure S6 XPS spectra of N doped C/Ni_5P_4/Fe_3P hollow nanocubes: (a) survey, (b) N 1s, (c) C 1s, (d) P 2p, (e) Ni 2p, and (f) Fe 2p.

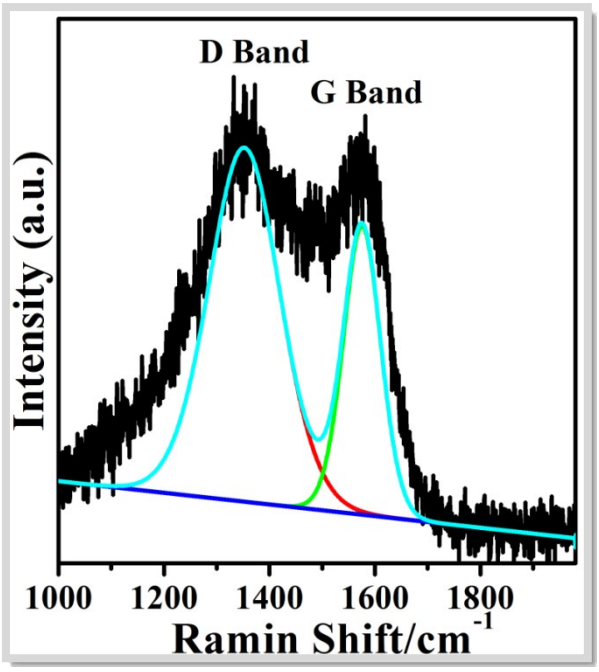

Figure S7 Raman spectrum of N-doped C coated Ni_5P_4/Fe_3P nanoparticles.

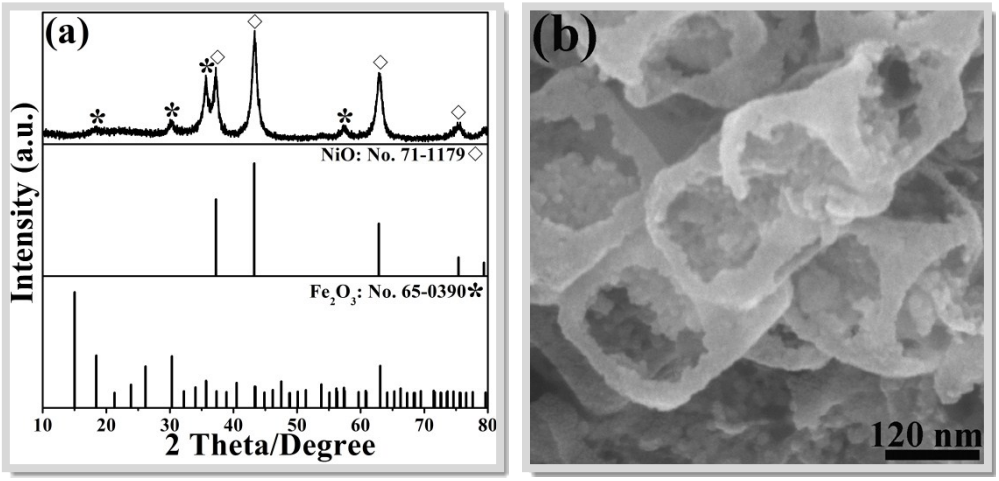

Figure S8 (a) XRD pattern and (b) SEM image of Fe_2O_3/NiO hollow nanocubes.

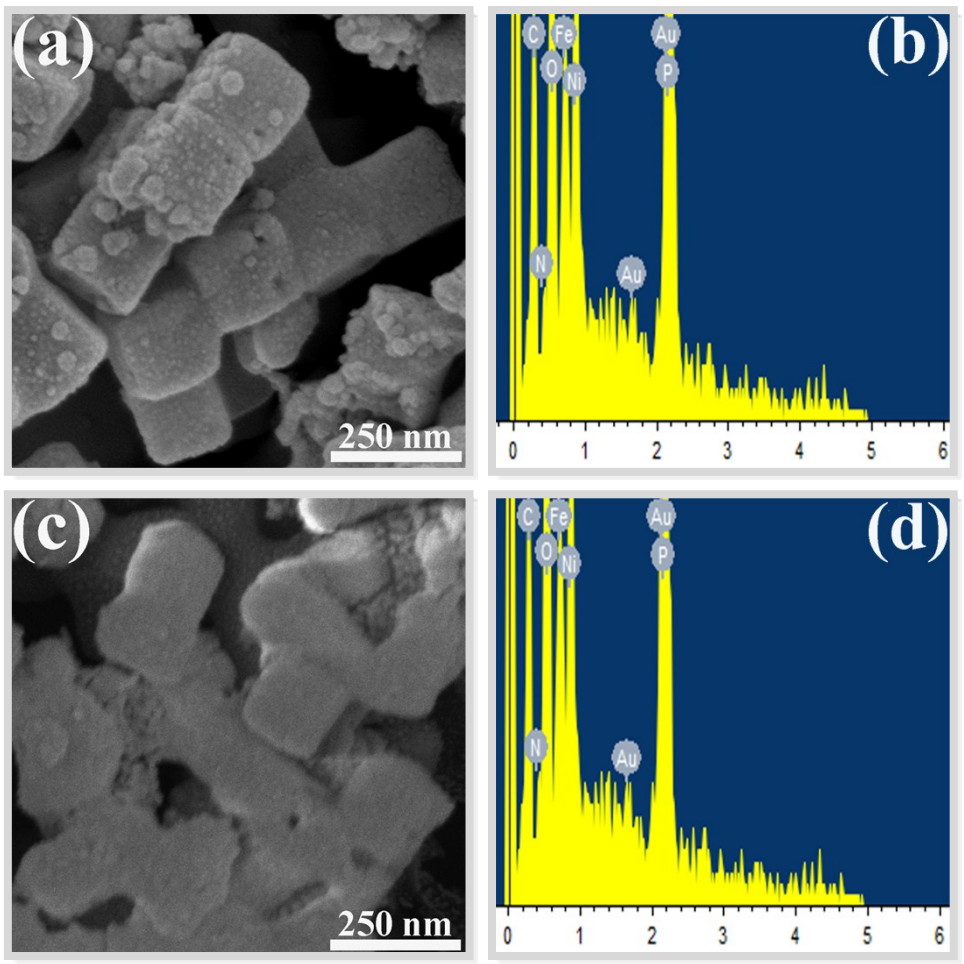

Figure S9 SEM images and EDS spectra of N doped C/Ni_5P_4/Fe_3P hollow nanocubes before (a-b) and after OER operations (c-d).

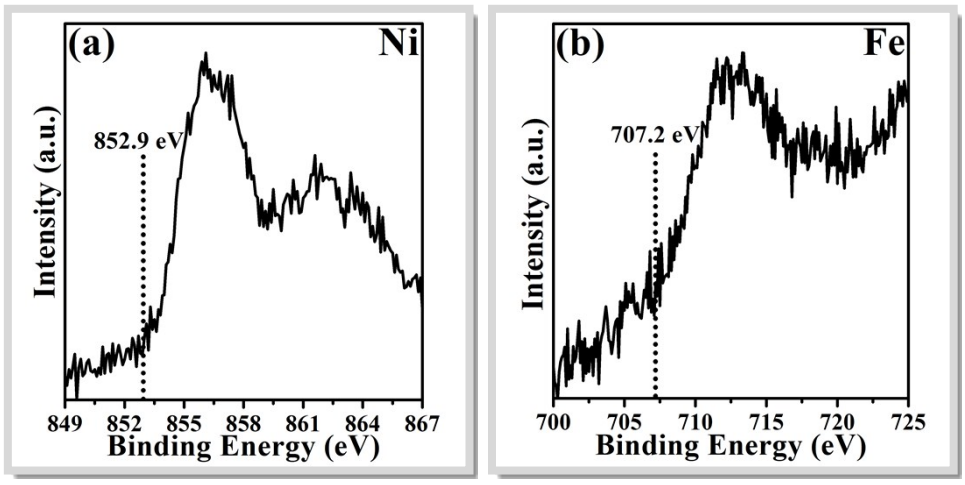

Figure S10 XPS spectra of N doped C/Ni_5P_4/Fe_3P hollow nanocubes after OER: (a) Ni and (b) Fe.

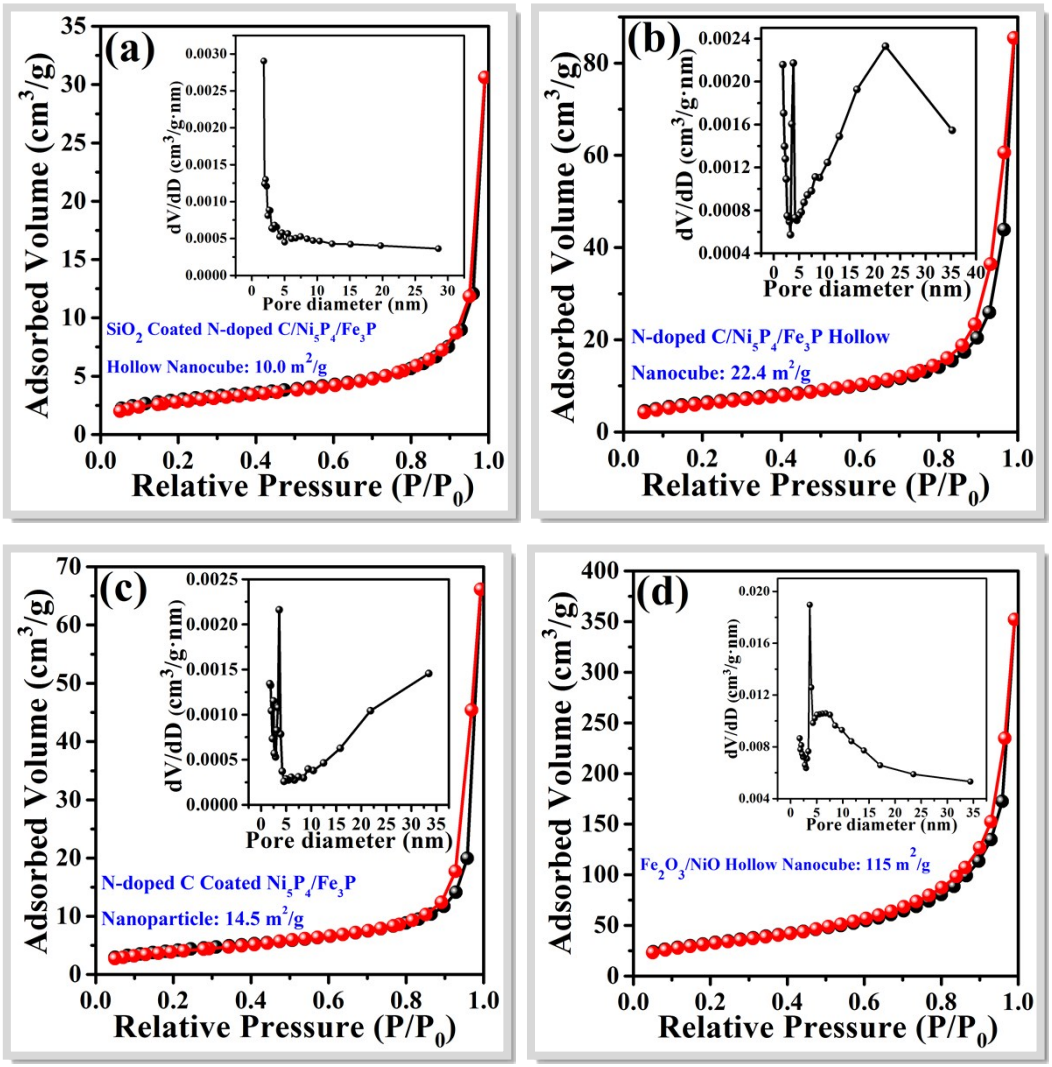

Figure S11 Nitrogen adsorption/desorption isotherms and corresponding pore-size distributions of (a) SiO_2 coated N-doped $C/Ni_5P_4/Fe_3P$ hollow nanocubes, (b) N-doped $C/Ni_5P_4/Fe_3P$ hollow nanocubes, (c) N-doped C coated Ni_5P_4/Fe_3P nanoparticles, and (d) Fe_2O_3/NiO hollow nanocubes.

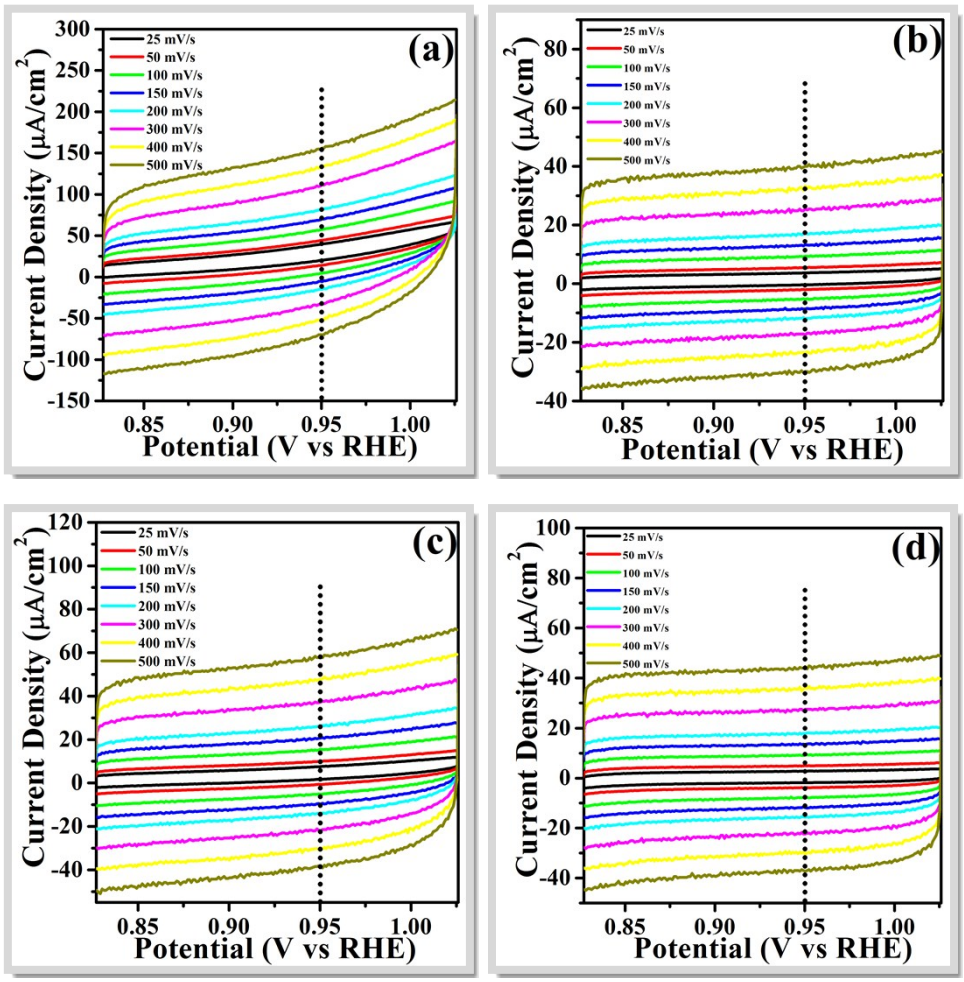

Figure S12 Cyclic voltammograms recorded at increasing scan rates in 1 M KOH:(a) N-doped C/Ni_5P_4/Fe_3P hollow nanocubes, (b) SiO_2 coated N-doped C/Ni_5P_4/Fe_3P hollow nanocubes, (c) N-doped C coated Ni_5P_4/Fe_3P nanoparticles, and (d) Fe_2O_3/NiO hollow nanocubes.

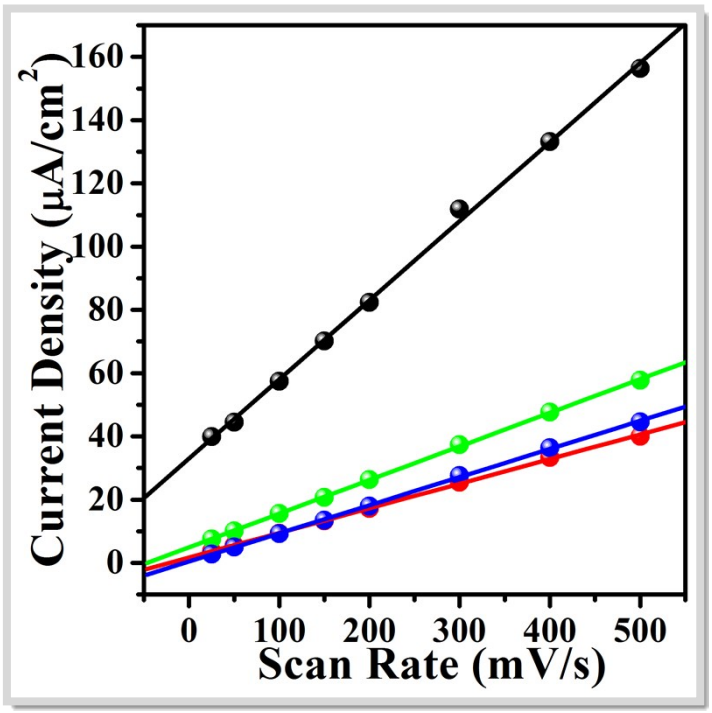

Figure 13 Linear fitting of capacitive current density achieved at 0.95 V vs. RHE *vs.* scan rate in 1.0 KOH: N-doped C/Ni_5P_4/Fe_3P hollow nanocubes (black), SiO_2 coated N-doped C/Ni_5P_4/Fe_3P hollow nanocubes (red), N-doped C coated Ni_5P_4/Fe_3P nanoparticles (green), and (d) Fe_2O_3/NiO hollow nanocubes (blue).

Table S1. Comparison of η_{10} and Tafel slope: present work *vs*. literature.

Catalysts	Loading Mass (mg/cm^2)	η_{10} (mV)	Tafel slope (mV/dec)	Reference
N doped C/Ni-P/Fe-P Hollow Nanocube	**0.5**	**252 (η_{20}= 276) (η_{50}= 305) (η_{100}= 332) (η_{250}= 385)**	**24**	**This work**
CoP/rGO	0.28	340 (η_{20}= 379)	66	*Chem. Sci*., 2016, 7, 1690-1695
Mn-Co oxyphosphide multi-shelled particle	0.25	320	52	*Angew. Chem. Int. Ed.*, 2017, 56, 2386-2389
NiCoP/C nanobox	N/A	330	96	*Angew. Chem. Int. Ed.*, 2017, 56, 3897-3900
CoMnP nanoparticle	0.28	330	61	*J. Am. Chem. Soc.*, 2016, 138, 4006-4009
CoPi-1	0.2	380	59	*Small*, 2016, 12, 1709-1715
Co-P foam	N/A	300	74	*J. Mater. Chem. A*, 2016, 4, 18272-18277
CoP_3 NAs/CFP	1	334 (η_{50}= 407)	62	*J. Mater. Chem. A*, 2016, 4, 14539-14544
NiCuP	N/A	292	49	*Nanoscale*, 2017, 9, 4401-4408
$Ni_{0.69}Co_{0.31}$-P	3.5	266	81	*Nanoscale*, 2016, 8, 19129-19138
np-$(Co_{0.52}Fe_{0.48})_2P$	1	270	30	*Energy Environ. Sci*., 2016, 9, 2257-2261
Ni-P	0.2	300	64	*Energy Environ. Sci*., 2016, 9, 1246-1250
Ni_2P	0.14	290	47	*Energy Environ. Sci*., 2015, 8, 2347-2351
CoP NP/C	0.71	320	99	*ACS Catal*., 2015, 5, 6874-6878
Co-Fe-P-1.7	0.424	260	58	*ACS Appl. Mater. Interfaces*, 2017, 9, 362-370
Cu_3P/CuO@NF	1.2	330	54	*ACS Appl. Mater. Interfaces*, 2017, 9, 2240-2248
Co_2P/CNT	2	292	68	*Nano Energy,* 2016, 30 303-311

$Cu_{0.3}Co_{2.7}P$/nitrogen-doped carbon	0.4	190	44	*Adv. Energy Mater.*, 2017, 7, 160155
Ni-Fe-P@C	N/A	217	40	*J. Mater. Chem. A*, 2017, 5, 2496-2503
NiFe-P catalyst	N/A	N/A (η_{20}= 204)	88	*J. Mater. Chem. A*, 2016, 4, 13866-13873
NiCuP	6.70	N/A (η_{50}= 300) (η_{100}= 318)	49	*Nanoscale*, 2017, 9, 4401-4408
NiSe/nickel foam	2.8	N/A (η_{20}= 270)	64	*Angew. Chem. Int. Ed.*, 2015, 54, 9351-9355
FeNi-rGO LDH hybrids	0.25	195	39	*Angew. Chem. Int. Ed.*, 2014, 53, 7584-7588